# Dalton Transactions



**PAPER** 

View Article Online



**Cite this:** *Dalton Trans.*, 2025, **54**, 11306

# Amino-functionalized cerium based MOF for sustainable CO<sub>2</sub> fixation into cyclic carbonates†

Yogesh Kumar, 📵 a Rishukumar Panday 📵 b and Shaibal Banerjee 📵 \*a

The conversion of  $CO_2$  into valuable chemicals is a pivotal strategy to mitigate environmental and energy challenges. In this context, we report the design and synthesis of a cerium-based metal-organic framework { $[Ce(L-NH_2)_{0.5}(NO_3)(H_2O)_2]\cdot 2DMF}$  ( $Ce-TPTC-NH_2$ ), constructed from Ce(III) centers and a precisely engineered amino-functionalized terphenyl tetracarboxylate ligand { $L-NH_2$ } ( $TPTC-NH_2$ ). This crystalline, microporous framework not only exhibits excellent catalytic performance in the solvent-free cycloaddition of  $CO_2$  with suitable epoxides, achieving >99% conversion under mild conditions (5 bar  $CO_2$ , 100 °C, 0.06 mol% catalyst) but also demonstrates unprecedented structural stability and reusability over multiple cycles. The synergistic interplay between Lewis acidic  $Ce^{3+}$  centers and basic  $-NH_2$  groups enables enhanced activation of both  $CO_2$  and epoxide substrates while lowering the activation barrier. Importantly, this Ce-MOF integrates bifunctional acid-base sites and is tailored specifically for  $CO_2$  fixation. The catalyst retained its crystallinity and >90% activity after five cycles, confirming its practical viability. This work introduces a design pathway for amine-functionalized Ce-MOFs, showcasing their potential as highly efficient, stable, and reusable heterogeneous catalysts for  $CO_2$  fixation under solvent-free conditions.

Received 6th April 2025, Accepted 30th June 2025 DOI: 10.1039/d5dt00825e

# Introduction

rsc li/dalton

The atmospheric CO<sub>2</sub> levels have significantly increased since the Industrial Revolution, leading to major environmental challenges. While CO<sub>2</sub> is essential for regulating Earth's temperature, its excessive emissions are driving climate change, highlighting the need for effective capture and utilization strategies. One promising approach is the catalytic conversion of CO2 into value-added chemicals, such as cyclic carbonates, which are widely used in the polymer and pharmaceutical industries. The cycloaddition of CO2 with epoxides offers a clean and practical route for converting exhaust carbon into useful chemicals, supporting the global pursuit of net-zero emissions. However, activating CO2 transformation presents a significant challenge due to the high bond enthalpy of the C=O bond (+805 kJ mol<sup>-1</sup>), making the choice of catalysts crucial for improving both the efficiency and scalability of the process.2 Heterogeneous catalysts, including zeolitic imidazolate frameworks,3 and transition-metal complexes4,5 have been

explored for CO<sub>2</sub> conversion, but their low catalytic stability, poor recyclability, and dependence on harsh reaction conditions (high temperature and high CO<sub>2</sub> pressure) limit their practical application. Additionally, these active sites often require high CO<sub>2</sub> loading, which can lead to reduced conversion efficiency and selectivity. Among the advanced materials, metal–organic frameworks (MOFs) have emerged as promising candidates for CO<sub>2</sub> adsorption.<sup>6–8</sup> Due to their high surface area, tunable porosity, and functionalizing ability, MOFs offer a unique platform for heterogeneous catalysis, as their structures can be tailored to incorporate catalytically active sites.<sup>1,9,10</sup> In particular, zirconium-based MOFs have demonstrated excellent stability; however, their synthesis typically requires high temperature and pressure, making large-scale production challenging.<sup>11,12</sup>

Recent research focus has shifted towards lanthanide-based MOFs, particularly cerium, for catalytic applications, primarily due to their large size and high coordination numbers. These frameworks exhibit excellent adsorption capacity, versatile redox behavior, and water stability. The latter arises from the highly acidic lanthanide centers that form strong coordination bonds with multidentate organic linkers, enhancing both the structural rigidity and the hydrophobic character of the material. Furthermore, the phenomenon of lanthanide contraction, arising from the poor shielding of the 4f orbitals, results in a gradual decrease in ionic radii across the series, leading to a higher effective nuclear charge. This increased

<sup>&</sup>lt;sup>a</sup>Department of Applied Chemistry, Defence Institute of Advanced Technology (DIAT), Pune 411025, India. E-mail: banerjeess@diat.ac.in

<sup>&</sup>lt;sup>b</sup>Department of Chemistry, Indian Institute of Science Education and Research, Pune, Dr. Homi Bhabha Road, Pashan, Pune - 411008, India

<sup>†</sup>Electronic supplementary information (ESI) available. CCDC 2429809. For ESI and crystallographic data in CIF or other electronic format see DOI: https://doi.org/10.1039/d5dt00825e

Lewis acidity enhances the metal centres' ability to coordinate with electron-rich substrates such as epoxides, thereby facilitating efficient catalytic activation. Cerium-MOFs are mostly favored due to their abundance, cost-effectiveness, and redoxactive Ce<sup>3+</sup>/Ce<sup>4+</sup> centers. 13-16 Unlike Zr-MOFs, Ce-MOFs can be synthesized under milder conditions while maintaining comparable catalytic activity and stability. These materials have been extensively studied in applications such as gas storage, energy conversion, and photocatalysis. 17-21 Recently, Ma et al. have synthesized lanthanide-based MOFs using cerium metal ions.<sup>22</sup> This MOF facilitates the removal of fluoride from water by adsorption. In another study, Lammert et al. have synthesized a series of Cerium-based MOFs, including various linker chains.<sup>23</sup> The produced MOFs have significant thermal stability and can serve as catalysts in many chemical conversions, including alcohol oxidation.<sup>23</sup> However, their potential in CO<sub>2</sub> conversion remains relatively underexplored.<sup>24-26</sup>

The design and synthesis of porous materials with welldefined functionalities remain a cornerstone of materials chemistry, particularly in the context of CO2 capture and conversion. In this work, we report the synthesis of a novel cerium-based metal-organic framework {[Ce(L-NH<sub>2</sub>)<sub>0.5</sub>(NO<sub>3</sub>) (H<sub>2</sub>O)<sub>2</sub>]·2DMF} (Ce-TPTC-NH<sub>2</sub>), constructed from an aminefunctionalized p-terphenyl-3,5,3',5'-tetracarboxylate {L-NH<sub>2</sub>} (TPTC-NH<sub>2</sub>) ligand. The synthesis yields a highly crystalline and stable framework, as confirmed by single-crystal X-ray diffraction (SCXRD). Further, microscopic analysis using highresolution transmission electron spectroscopy (HR-TEM), X-ray photoelectron spectroscopy (XPS), field-emission scanning electron microscopy (FE-SEM), and temperature-programmed desorption (TPD) establishes its composition, porosity, morphology, and CO2 adsorption capacity. To enhance catalytic efficiency, amine (-NH2) functionalization was introduced, as NH2 groups act as Lewis-basic sites, facilitating CO<sub>2</sub> interactions and improving electronic properties. Ce-TPTC-NH<sub>2</sub> features a  $\pi$ -conjugated terphenyl core that enhances framework stability and electronic interactions, while the amine (-NH<sub>2</sub>) moieties facilitate strong acidbase interactions, improving CO2 affinity and catalytic efficiency;27-30 Cerium was selected as the metal center due to its redox-active nature (Ce3+/Ce4+), high Lewis acidity, and strong affinity for oxygen-donor ligands. Additionally, the strong coordination between the highly charged Ce<sup>3+</sup> ions and the tetra carboxylate TPTC ligand imparts hydrophobic character to the framework, enhancing its resistance to hydrolysis. The coexistence of Lewis-acidic Ce metal sites and basic amine groups creates a synergistic effect, enabling efficient  $CO_2$  activation and conversion.  $^{31-33}$ 

The catalytic efficiency of Ce-TPTC-NH2 is demonstrated in the solvent-free cycloaddition of CO<sub>2</sub> with epoxides, achieving >99% conversion. Moreover, Ce-TPTC-NH<sub>2</sub> exhibits good recyclability, retaining its catalytic activity over five consecutive cycles without significant degradation. Compared to previously reported Ce-MOFs, Ce-TPTC-NH<sub>2</sub> exhibits superior CO<sub>2</sub> affinity and catalytic efficiency, establishing it as a highly effective and reusable platform for sustainable CO<sub>2</sub> utilization.<sup>34</sup>

# Results and discussion

The Ce-TPTC-NH2 MOF was synthesized by the solvothermal reaction of TPTC-NH2 ligand and Ce(NO3)3.6H2O in dimethyl formamide (DMF) solvent. The TPTC-NH2 ligand was synthesized with modifications to previously reported procedures (Schemes 1 and 2).35

In order to understand the synergistic effect of Ce-TPTC-NH<sub>2</sub> catalyst for CO<sub>2</sub> capture and conversion. First, the structural and electronic properties of Ce-TPTC-NH2 MOF were systematically analyzed through various spectroscopic techniques to elucidate the role of amino functionalization in optimizing these functionalities.

Single-crystal X-ray diffraction analysis revealed that Ce-TPTC-NH<sub>2</sub> crystallizes in the monoclinic system with a C2/c space group. The asymmetric unit shown in Fig. 1a consists of one crystallographic unit Ce(III) atom, a symmetrically half-unit of the TPTC-NH2 ligand, where the -NH2 group is disordered over two positions, one NO<sub>3</sub><sup>-</sup> anion, two coordinated water molecules, and two free DMF molecules. A detailed examination of the coordination environment indicates that Ce-TPTC-NH<sub>2</sub> forms dinuclear Ce<sub>2</sub> clusters, in which pairs of Ce (III) ions are bridged by four carboxylate groups from four distinct TPTC-NH2 ligands (Fig. 1b). The coordination sphere of the Ce(III) ions is completed by disordered nitrate ions and two coordinated water molecules. The TPTC-NH2 ligands, in turn, connect to four separate Ce2 dimers. The overall 3D network can be simplified by considering both the Ce2 dimers and TPTC-NH<sub>2</sub> ligands as 4-connecting nodes (Fig. 1c). The powder X-ray diffraction (PXRD) patterns of the simulated and as-synthesized Ce-TPTC-NH2 exhibit strong correspondence, signifying its phase purity. The PXRD pattern of the Ce-TPTC-NH2 samples is shown in Fig. 1d, displaying significant diffraction peaks at roughly  $2\theta$  values of 7.08°, 8.95°, 9.80°, and 17.51°, corresponding to the (200), (004), (112), and (204) planes,

Scheme 1 Synthetic pathway of TPTC-NH<sub>2</sub> by Suzuki coupling reaction.

Scheme 2 Synthetic pathway of Ce-TPTC-NH<sub>2</sub>

Paper Dalton Transactions

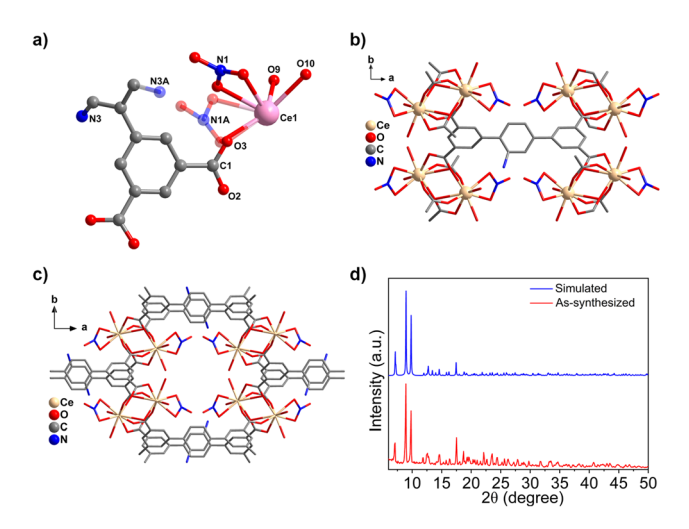


Fig. 1 (a) The asymmetric unit of  $Ce-TPTC-NH_2$  MOF. (b) The second building unit for the dinuclear  $Ce_2$  cluster. (c) Packing along the c-axis, (d) PXRD pattern of the synthesized  $Ce-TPTC-NH_2$  MOF in comparison to the simulated pattern.

respectively. The XRD patterns of all samples demonstrate a significant degree of crystallinity. Furthermore, the crystallite sizes of the samples were  $\sim$ 55 nm on average, which was calculated using the main XRD peaks and the Scherrer equation via Xpert High Score-Plus software64.

$$D = (K\lambda)/(\beta \cos \theta)$$

*D* is the average size of crystallites, *K* is the shape factor,  $\lambda$  is X-ray wavelength,  $\beta$  is full width at half maximum (FWHM) of the diffraction peak in radian, and  $\theta$  is Bragg angle.

Field Emission Scanning Electron Microscopy (FE-SEM) was employed to observe the morphology of the synthesized crystals of Ce-TPTC-NH<sub>2</sub>. In Fig. 2a, the image of Ce-TPTC-NH<sub>2</sub> reveals a cluster of thick and pillared layered crystals with a size of 1–2 µm. Besides, the detailed analysis of energy-dispersive X-ray spectroscopic (EDS) results in Fig. 2b confirms the presence of Ce, O, C, and N within the synthesized compound. Ce-TPTC-NH<sub>2</sub> had an optimal cerium content (16.42%), as shown in Fig. 2c, which is consistent with other reported cerium-based MOFs.<sup>22</sup>

To further explore the coordination interaction between all the elements, present in the **Ce-TPTC-NH<sub>2</sub>**, the XPS analysis results are presented in Fig. 3a–c. The XPS spectra of Ce(III)  $3d_{5/2}$  and  $3d_{3/2}$  regions for **Ce-TPTC-NH<sub>2</sub>** are deconvoluted into four components, attributed to the formation of Ce(III) oxocluster, appearing between 882 and 904 eV (Fig. 3a). The high-resolution O 1s spectra exhibit peaks at 532.18 eV, attributed to hydroxyl bonding to metal (M–OH), and another peak at 533.58 eV, assigned to metal oxide (M–O) (Fig. 3b). This slight shift of C—O at 533 eV indicates the bonding of oxygen with cerium metal ions. The N 1s spectrum shows peaks at 400.57 eV, corresponding to the free (–NH<sub>2</sub>) amine peak, whereas the peak at 403.08 and 407.38 eV corresponds to N–C—O of DMF bound to cerium metal ion, and nitrate ions from nitric acid,

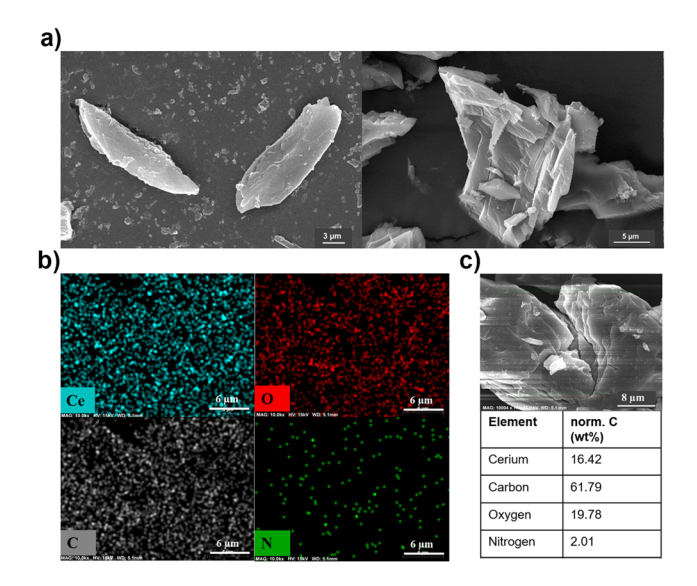


**Fig. 2** (a) FE-SEM images, (b) elemental mapping, and (c) SEM-EDX elemental analyses of **Ce-TPTC-NH**<sub>2</sub> MOF.

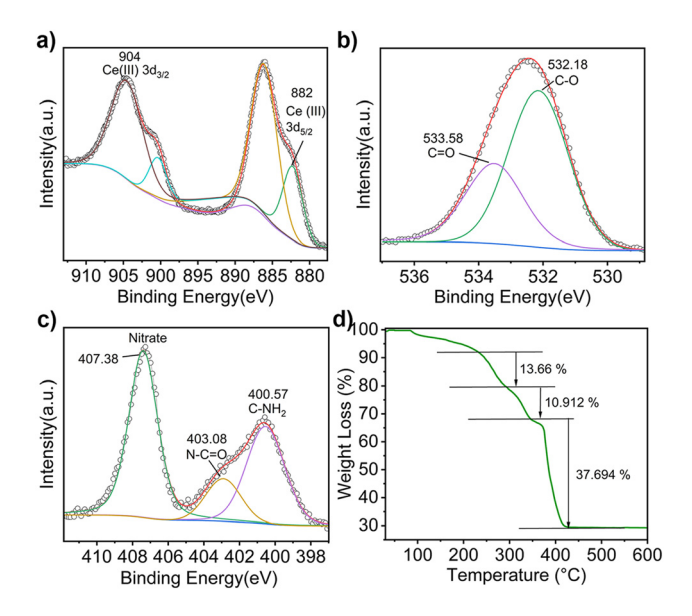


Fig. 3 XPS deconvolution spectra of the (a–c) Ce 3d, O 1s, and N 1s (d) TGA analysis of Ce-TPTC-NH $_2$  MOF.

respectively. The shift in the binding energy of N-C=O and nitrate ions towards higher energy can be attributed to electronic conjugation within the framework following MOF synthesis (Fig. 3c). The C 1s spectrum has peaks at 284.94, 286.44, and 288.70 eV, corresponding to C-C, C-O-C, and O-C=O, respectively (Fig. S4†). The analysis of the peak integrations from the XPS spectrum indicates that the atomic fractions of O 1s, Ce 3d<sub>5</sub>, C 1s, and N 1s in Ce-TPTC-NH<sub>2</sub> are 33, 2.74, 55.75, and 8.51%, respectively.

To evaluate the thermal stability of Ce-TPTC-NH<sub>2</sub>, thermogravimetric analysis (TGA) measurement was performed as shown in Fig. 3d. Thermogravimetric analysis of Ce-MOF

shows the initial weight loss before 200 °C should be associated with water molecules coordinated with the MOF. The weight loss in temperature ranging from 200 °C to 300 °C should be attributed to the decomposition of coordinated DMF molecules.<sup>35</sup> A substantial % weight loss of 37% appeared in the temperature range of 380-420 °C, suggesting the collapse of the frameworks and decomposition of the organic ligands. Furthermore, TGA validated the thermal robustness of Ce-TPTC-NH2 up to 380 °C. The BET surface area of the Ce-TPTC-NH2 MOF was measured and found to be similar to that of a previously reported europium-based MOF (Fig. S5†).

The strength and distribution of acidic and basic sites that facilitate reactant activation on synthesized materials were evaluated using NH<sub>3</sub>-TPD (TPD = temperature-programmed desorption) and CO<sub>2</sub>-TPD, <sup>36</sup> respectively, as seen in Fig. 4. The sample exhibited a desorption pattern between 100 °C and 700 °C. Acidic and basic sites in a catalyst are often categorized as weak (100-250 °C), moderate (250-450 °C), and strong (>450 °C). These peaks result from the distinct physical and chemical adsorption of CO2 and NH3.

The intense peak at about 300 °C in CO<sub>2</sub>-TPD is linked to the existence of free amine sites, highlighting the impact of the (-NH<sub>2</sub>) moiety inserted in the ligand (Fig. 4a). Simultaneously, the NH<sub>3</sub>-TPD profile is seen in Fig. 4b. Adsorption of NH<sub>3</sub> at Cesites has been suggested to give rise to the intense desorption peak observed at 250-350 °C.37 The graph demonstrates that the amine-functionalized Ce-TPTC-NH2 MOF possesses strong basic sites (0.940 mmol  $g^{-1}$ ) and acidic sites (0.956 mmol  $g^{-1}$ ), facilitating the activation of the epoxide ring and CO<sub>2</sub> molecule (Table 1). The synergistic effect of Lewis acidic Ce(III) sites and basic amine (-NH2) functionalities through TPD studies, highlighting their role in CO<sub>2</sub> activation.

The stability of Ce-TPTC-NH2 was also observed in a series of solvents such as DMF, di-methyl sulfoxide (DMSO), methanol, ethanol, tetrahydrofuran (THF), boiling water, and DI water for 24 h. To further assess its chemical robustness, the MOF was soaked in mildly acidic (pH 5) and basic (pH 9) aqueous solutions. Meanwhile, the post-PXRD patterns of Ce-TPTC-NH2 remained almost the same as those of the as-synthesized Ce-TPTC-NH2, with a slight reduction in intensities confirming its stability (Fig. S6†). 24,25 Contact angle measure-

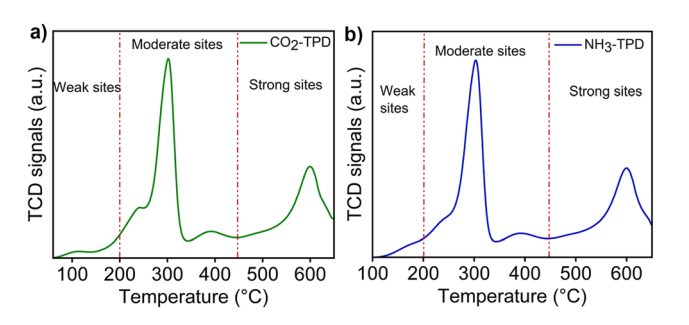


Fig. 4 Temperature-programmed desorption (TPD) (a) CO<sub>2</sub> and (b) NH<sub>3</sub> of Ce-TPTC-NH<sub>2</sub> MOF.

Table 1 Basic and acidic sites of Ce-TPTC-NH<sub>2</sub> determined by CO<sub>2</sub> and NH<sub>3</sub> temperature-programmed desorption

Property	Ce-TPTC-NH <sub>2</sub>
Weak basic sites (<250 °C) Moderate basic sites (250–450 °C) Strong basic sites (>450 °C) Total basic sites Weak acidic sites (<250 °C) Moderate acidic sites (250–450 °C) Strong acidic sites (>450 °C) Total acidic sites	0.265 mmol g <sup>-1</sup> (250 °C) 1.009 mmol g <sup>-1</sup> (300 °C) 0.940 mmol g <sup>-1</sup> (600 °C) 2.214 mmol g <sup>-1</sup> 0.236 mmol g <sup>-1</sup> (240 °C) 1.077 mmol g <sup>-1</sup> (300 °C) 0.956 mmol g <sup>-1</sup> (600 °C) 2.269 mmol g <sup>-1</sup>
Total acidic sites	2.269 mmol g <sup>-1</sup>

ment also supported the stability of Ce-TPTC-NH<sub>2</sub> MOF in polar solvents (Fig. S7†).

#### Catalytic activity: cycloaddition reaction of epoxide with CO<sub>2</sub>

Following activation, Ce-TPTC-NH2 was evaluated as a heterogeneous Lewis acid-base catalyst for the CO<sub>2</sub> with epoxide cycloaddition reaction. Its catalytic efficiency was systematically investigated through a series of experiments. 1-Chloro-2,3-epoxy propane (epichlorohydrin) was selected as the primary epoxide system in the coupling reaction with CO<sub>2</sub> under solvent-free conditions. A controlled experiment without a catalyst showed negligible conversion at 5 bar CO2 even after 24 hours. A series of experiments using Ce-TPTC-NH<sub>2</sub> MOF as a catalyst demonstrated significantly enhanced performance, achieving 99.9% selectivity for cyclic carbonates in CO2 conversion with good yield. NMR monitoring revealed that most conversions occurred within 12 hours, with no significant progress afterward.

We further investigated the reaction conditions by modifying parameters such as catalyst dosage, temperature, and duration, as shown in Fig. 5 and Table 2. A 10 mg (~0.0168 mol% of Ce) catalyst loading achieved ~98% epoxide

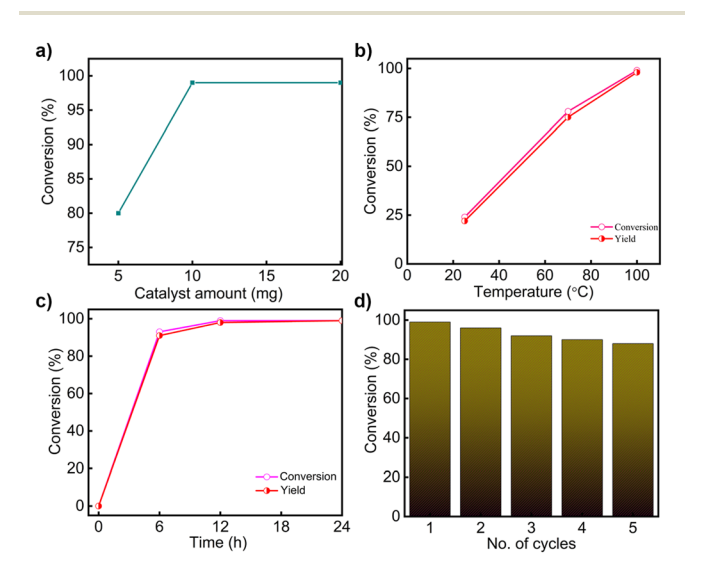


Fig. 5 Catalytic conversion of CO<sub>2</sub> by varying (a) catalyst amount, (b) temperature, (c) time, and (d) reusability study of catalytic conversion of CO<sub>2</sub> by Ce-TPTC-NH<sub>2</sub> MOF.

Paper **Dalton Transactions** 

Table 2 Catalytic activity of Ce-TPTC-NH2 for the cycloaddition reaction of CO<sub>2</sub> to cyclic carbonate

where, TBAB = t-butylammonium bromide

Entry	Ce-TPTC-NH <sub>2</sub> / TBAB ratio	Temp. (°C)	Time (h)	Conversion (%)	Yield (%)
1	0/0	100	24	10	3
2	20/0	100	24	40	17
3	0/16	100	24	23	16
4	20/16	100	12	99	99
5	10/16	100	24	99	99
6	10/16	100	12	99	98
7	20/16	70	12	84	82
8	20/16	70	24	86	83
9	10/16	70	12	78	75
10	10/16	70	24	80	73
11	20/16	rt	24	24	22
12	10/16	rt	24	18	17

Ce-TPTC-NH2 (10 mg), TBAB (16 mg), epoxide (2 mL), CO2 pressure (5 bar), temperature (100 °C), Time (12 h).

conversion to cyclic carbonate within 12 hours at 100 °C. Given the high yield, this loading was chosen for further optimization. The catalytic reaction was monitored using the <sup>1</sup>H-NMR spectrum, with the disappearance of the characteristic signal of epichlorohydrin at 3.2 ppm and the appearance of a signal at 4.9 ppm for cyclic carbonate (Fig. S8†). This analysis confirms that Ce-TPTC-NH2 is an efficient catalyst for CO2-to-epichlorohydrin coupling, achieving 99.9% selectivity. Since temperature plays a crucial role in the catalytic process, lowering the reaction temperature from 100 °C to 70 °C reduces the product yield from 98% to 75%, likely due to the enhanced CO2 incorporation into the C-O bond of oxidized epichlorohydrin at higher temperatures (Table 2). Given that CO<sub>2</sub> cycloaddition is exothermic, the optimal reaction temperature for Ce-TPTC-NH2 MOF-catalyzed CO2 cycloaddition is determined to be 100 °C, underscoring its high catalytic efficiency.

The cycloaddition procedure yielded 97% of 4-(chloromethyl)-1,3-dioxolan-2-one product utilizing 80% CO2. Ce-TPTC-NH2 as a catalyst facilitates the cycloaddition of CO2 and epoxides through a cooperative Lewis acid-base mechanism. The Ce<sup>3+</sup> centers activate the epoxide *via* coordination with its oxygen atom, while the Br anion from TBAB acts as a nucleophile to promote ring opening. The enhanced catalytic activity of Ce-TPTC-NH2 MOF with co-catalyst tetra-butyl ammonium bromide (TBAB) arises from the synergistic interaction between cerium Lewis acidic sites and basic bromine functionality. To investigate the influence of the nucleophile on catalytic performance, three co-catalyst systems: tetrabutylammonium bromide (TBAB), chloride (TBAC), and iodide (TBAI), in the presence of the Ce-TPTC-NH2 catalyst, were compared. Although the Br anion is moderately nucleophilic, it resulted in the highest conversion (98%), outperforming even the more nucleophilic I (68%) and Br system (17%). 25 Br offers an optimal balance between nucleophilicity and leaving group ability, making it more effective than Cl or I in similar systems. A control reaction without TBAB resulted in a significantly lower conversion (~17%), confirming its essential role. Given its mechanistic compatibility, stability, and literature precedence, TBAB was found to be the most appropriate co-catalyst for this system.

To further validate the role of basic sites in catalysis, we synthesized {[Ce(L)<sub>0.5</sub>(NO<sub>3</sub>)(H<sub>2</sub>O)<sub>2</sub>]·2DMF} (Ce-TPTC) following a previously reported procedure (Fig. S9†).22 As anticipated, Ce-TPTC, when used as a catalyst in combination with the cocatalyst TBAB, yielded a lower product conversion of approximately 65% with epichlorohydrin under the same reaction conditions employed for Ce-TPTC-NH2. Once the optimum reaction conditions (5 atm CO2, 12 h, 100 °C) were achieved for epichlorohydrin-to-cyclic carbonate conversion, we further tested the catalytic performance of Ce-TPTC-NH2 with a variety of epoxide substrates, including 2-methyloxirane, 2-propyloxirane, and 2-phenyloxirane, ranging from aliphatic to aromatic substituents.

The conversion and yield decrease as the epoxide substituent size increases, likely due to steric hindrance and electronic effects.<sup>25</sup> Bulkier epoxides with longer chains can obstruct the pores of Ce-TPTC-NH2, slowing down reactant diffusion and reducing efficiency. Selectivity for the cyclic carbonate products was >99% in all instances. All cyclic carbonate products

Table 3 Comparison of Ce-TPTC-NH<sub>2</sub> with other heterogeneous catalysts in the cycloaddition of CO<sub>2</sub> to cyclic carbonate

Material	Dosage	Pressure	Temperature	Co-catalyst	Cycles	Conversion	Ref.
MIL-101(Cr)-IP	42 mg	0.8 MPa	50 °C	_	_	91%	38
HPC-800	30 mg	0.15 bar	RT	TBAB	3	90%	39
PNU-25-NH <sub>2</sub> /TBAB	1 mol%	1 bar	55 °C	TBAB	4	92%	26
NH <sub>2</sub> -Ce-MUM-2	20 mg	1 atm	50 °C	TBAB	6	93%	24
Gd-TPTC-NH-[BMIM]Br	20 mg	0.1 MPa	100 °C	TBAB	5	91%	40
$Zr(H_4L)$	0.1 mmol	9.8 atm	100 °C	TBAB	5	>99%	41
Ce <sub>2</sub> NDC <sub>3</sub>	15 mg	0.1 MPa	RT	TBAB	5	89%	42
Ce(HTCPB)	0.0145 mmol	10 bar	100 °C	TBAB	3	97%	43
Meim-UiO-66	50 mg	0.1 MPa	120 °C	_	6	46%	44
Gd-TPTC-NH <sub>2</sub>	20 mg	0.1 MPa	100 °C	TBAB	_	31%	40
Ce-TPTC-NH <sub>2</sub>	20 mg	5 atm	100 °C	TBAB	5	>99%	This work

Table 4 Synthesis of cyclic carbonates from CO<sub>2</sub> and epoxides catalysed by Ce-TPTC-NH<sub>2</sub>

Sr. no.	Epoxide substrate	Product	Structure Type	Time (h)	Conversion (%)	Yield (%)
1	CI		Aliphatic terminal	12	99%	98%
	2-(chloromethyl)oxirane	CI				
		4-(chloromethyl)-1,3-				
2	0	dioxolan-2-one O	Aliphatic terminal	12	93%	89%
2			Anphatic terminal	12	93 70	0970
		0 0				
	2-methyloxirane					
		4-(methyl)-1,3-dioxolan-2-				
3	0	one O	Linear aliphatic terminal	12	94%	91%
		No.	Zinear anphaere terminar		31,0	3170
		0				
	2-propyl oxirane	~ \				
		4-(propyl)-1,3-dioxolan-2-				
4	٨	one O	Aromatic terminal	24	88%	69%
	2-phenyl oxirane	4/1 1/42 1/42				
		4-(phenyl)-1,3-dioxolan-2- one				
5		0	Six-membered internal	24	<12%	_
	1,2-Epoxycyclohexane	4,5 Tetramethylene-1,3-				
	~	dioxolane-2-one				
6	$\bigcirc$	√ b=0	Five membered internal	24	~20%	_
		\ <u>\</u> 0'				
	1,2-Epoxycyclopentane	tetrahydro-4H-				
		cyclopenta[d][1,3]dioxol-				
		2-one				

have been previously documented, and the data presented in Table 4 align with the existing literature. Although 2-propyloxirane carries a bulkier substituent, the initially lower yield observed with 2-methyloxirane is likely attributed to its higher volatility under solvent-free conditions at 100 °C, resulting in partial loss during the reaction. To validate this, the experiment was repeated with 2-methyloxirane, and by cooling the reaction mixture to 0 °C prior to product extraction, the isolated yield significantly improved to 89%, supporting the volatility-related explanation.

The durability and reusability of the Ce-TPTC-NH2 catalyst were assessed through successive cycloaddition reactions of epoxides and CO2 under optimized conditions. The catalyst was recovered via centrifugation, washed thoroughly with ethyl acetate, and dried at 70 °C overnight. Ce-TPTC-NH2 exhibited remarkable durability, retaining ~90% of its catalytic activity even after five cycles while maintaining high selectivity. The stability of parent and reused Ce-TPTC-NH2 samples was confirmed using PXRD and HR-TEM analysis. The PXRD patterns after five catalytic cycles showed that the crystallinity of the MOF was retained, with a slight decrease in peak intensity (Fig. S10†). The HRTEM images revealed that the morphology and particle integrity were well preserved, with no visible aggregation, collapse, or structural degradation before and

**Paper Dalton Transactions** 

after catalysis (Fig. S11†). The HRTEM analysis of the as-synthesized Ce-TPTC-NH2 MOF revealed a uniform particle morphology with an expected particle size in the range of 1-2 μm, as referred to by dynamic light scattering (DLS) experiment data (Fig. S12†).

However, after five cycles, the conversion efficiency declined to ~85%, likely due to partial blockage of active sites. Additionally, complete catalyst recovery was not achieved, potentially due to minor losses during filtration and washing, structural degradation, or partial leaching of active species. To assess the extent of cerium leaching, the post-reaction filtrate was analyzed by microwave plasma-atomic emission spectroscopy (MP-AES). The initial Ce content in the catalyst before catalysis was determined to be 63 ppm in a 100 ppm dispersion, which slightly decreased to 58 ppm after the fifth cycle. This minor decrease indicates negligible Ce leaching (~7.9%), confirming the structural robustness and recyclability of the catalyst under the applied reaction conditions. The catalytic performance of Ce-TPTC-NH2 was compared with selected MOF and organocatalyst systems reported in the literature (see Table 3).

#### Proposed mechanism of CO<sub>2</sub> conversion

The cycloaddition of CO<sub>2</sub> with epoxides to form cyclic carbonates, catalyzed by Ce-TPTC-NH<sub>2</sub>, follows a plausible synergistic activation mechanism involving Lewis acidic Ce(III) centers and nucleophilic amino (-NH<sub>2</sub>) functional groups (Fig. 6). However, activating CO<sub>2</sub> transformation requires significant energy due to the high bond enthalpy of the C=O bond (+805 kJ mol<sup>-1</sup>). The catalytic cycle begins with electron-rich amine (-NH<sub>2</sub>) group acting as Lewis base, interacting with the carbon atom of CO2 and stabilizing its acidic nature.

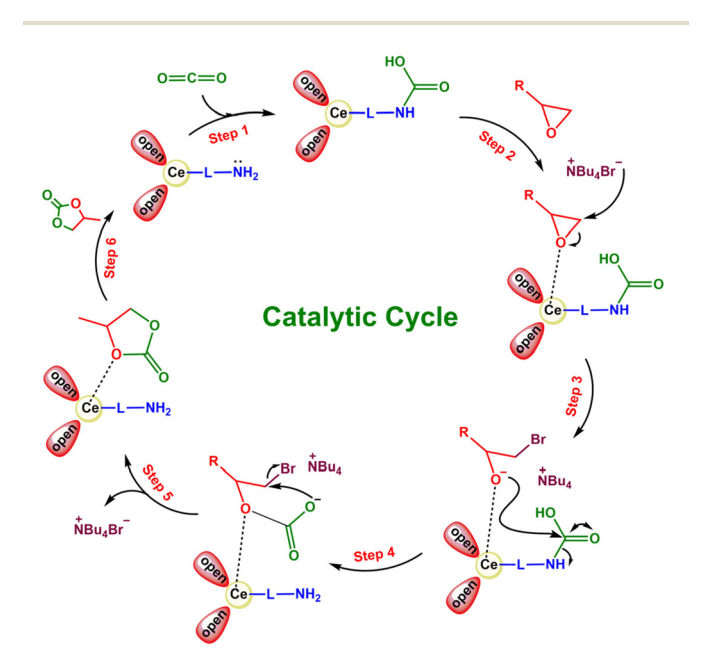


Fig. 6 Catalytic cyclic process of conversion of epoxide into cyclic carbonate.

Simultaneously, the Lewis-acidic Ce(III) centers coordinate with the oxygen atom of the epoxide, increasing its electrophilicity. In the second step, the Br anion, generated from TBAB (cocatalyst), then initiates a nucleophilic attack on the activated epoxide, leading to the formation of an alkoxide-metal intermediate. Subsequently, CO2 insertion into this alkoxide complex promotes intramolecular cyclization, yielding a fivemembered cyclic carbonate. In the final step, the bromide ion is released and reintegrated into the catalytic cycle, ensuring continuous turnover of the active Ce(III) species. The cyclic carbonate product detaches from the metal center, preserving the catalyst integrity and allowing for successive reaction cycles with minimal deactivation. 40,45 This catalytic system demonstrates excellent activity and selectivity in cyclic carbonate synthesis, offering a sustainable and efficient route for CO2 utilization. Operating under ambient to mild conditions with a reusable catalyst aligns with green chemistry principles, converting CO2 into valuable chemical products. Integrating CO2 as a feedstock mitigates greenhouse gas emissions and advances sustainable carbon valorization, paving the way for practical and environmentally benign CO2 conversion strategies.

# **Experimental**

#### **Materials**

Cerium(III) nitrate hexahydrate (Reacton™, 99.5%) was purchased from Alfa Aesar. (3,5-Bis(methoxy carbonyl)phenyl) boronic acid, palladium acetate (Pd(OAc)2), 2,5-dibromoaniline (>98%), tetrabutyl ammonium bromide (TBAB), and cesium carbonate (Cs<sub>2</sub>CO<sub>3</sub>) were purchased from Sigma-Aldrich. Dimethyl formamide (DMF) and nitric acid (69%) were purchased from Merck.

## Synthetic procedure

Synthesis of 2'-amino-1,1':4',1"-terphenyl-3,5,3',5'-tetracarboxylic acid (TPTC-NH<sub>2</sub>). The synthesis was performed following a modified procedure as shown in Scheme 1.46 First, tetramethyl 2'-amino-[1,1':4',1"-terphenyl]-3,3",5,5"-tetracarboxylate (Me<sub>4</sub>L-NH<sub>2</sub>) was synthesized under nitrogen atmosphere. A mixture of 3,5-bis methoxy carbonyl phenylboronic acid (0.238 g, 1 mmol), 2,5-dibromo aniline (0.063 g, 0.25 mmol),  $Pd(OAc_2)_3$  (0.0015 g, 0.0067 mmol) and  $Cs_2CO_3$  (0.325 g, 1 mmol) was added to a solution of deoxygenated N,N-dimethylformamide (8 mL) and water (10 mL) in a 100 mL two neck round bottom flask, which was then refluxed at 105 °C for 12 hours. The reaction was allowed to cool at room temperature, and the greenish-yellow mixture was extracted with ethyl acetate and brine water three times; ethyl acetate was dried over anhydrous Na2SO4 and removed under reduced pressure. Further purification of compound Me<sub>4</sub>L-NH<sub>2</sub> was done by column chromatography (EtOAc:hexane = 30:70 by volume;  $R_f$ : 0.38), yielding a light-yellow compound (0.286 g, 0.6 mmol). Yield: 64%. <sup>1</sup>H NMR (400 MHz, DMSO-D<sub>6</sub>),  $\delta$  = 8.68 (d, 2 H), 8.48 (s, 2H), 8.39 (s, 2H), 7.24 (s, 1H), 7.15 (d, 1H), 7.08 (s, 1H), 3.98 (d, 12H) ppm.

Tetramethyl 2'-amino-[1,1':4',1"-terphenyl]-3,3",5,5"-tetra carboxylate (0.286 g, 0.6 mmol) was then suspended in THF (10 mL) for 30 minutes, to which 20 mL of 5.50 M KOH in an aqueous ethanol solution was added. The mixture was stirred under reflux overnight at 65 °C. The reaction was allowed to cool at room temperature and centrifuged to collect the precipitates. The precipitates were then suspended to 10 mL THF, followed by a dropwise addition of dilute HCl until the solution pH reached 2-3. Excess water was added to the mixture to achieve the quick precipitation of a light-yellow solid as the product. The solid was collected by filtration, washed with water, and dried to give TPTC-NH<sub>2</sub> (Fig. S1–S3†). Yield: 93.2%.  $^{1}$ H NMR (400 MHz, DMSO-D<sub>6</sub>):  $\delta$ = 8.40 (d, J = 1.4 Hz, 2H), 8.33 (s, 1H), 8.17 (s, 2H), 7.49 (s, 2H)1H), 7.35 (d, 1H), 7.21 (d, 1H), 3.15 (d, 2H). m/z (ESI-MS) [M - H]: 422.08. Elemental analysis (%) calc.: C, 62.71; H, 3.59; N, 3.32; O, 30.38.; found: C, 62.51; H, 3.89; N, 3.22; O, 30.18.

#### Synthesis of Ce-TPTC-NH<sub>2</sub> MOF

The synthesis of MOF Ce-TPTC-NH2 was performed following a modified procedure (Scheme 2).22 A mixture of Ce (NO<sub>3</sub>)<sub>3</sub>·6H<sub>2</sub>O (0.130 g, 0.3 mmol) and TPTC-NH<sub>2</sub> (42 mg, 0.1 mmol) was dissolved separately in DMF (10 mL) and added to a screw-capped vial. Further, two drops of HNO<sub>3</sub> (65%, aq) were added to the mixture. The vial was sealed and placed in a preheated oven at 105 °C for 24 hours. Crystals were obtained after 48 hours and air-dried. Yield: 59% (based on TPTC-NH2 ligand). The solvent exchange was carried out for three days with fresh acetone every day.

## General procedure of catalytic coupling of epoxide and CO<sub>2</sub>

Before the catalytic test, Ce-TPTC-NH2 MOF was activated by heating at 100 °C under vacuum to remove the guest solvent. The reaction was carried out in a stainless-steel high-pressure reactor, where (2 mL, 25.3 mmol) of the epoxide was added along with 0.06 mol% of catalyst and (16 mg, 0.5 mmol) TBAB. The reactor was sealed and purged with 5 bar CO<sub>2</sub>. The temperature was maintained at 100 °C under stirring for 24 h. Upon completion, the reaction mixture was cooled to 0 °C, and a small aliquot was taken for catalyst separation via centrifugation. The crude product was purified using column chromatography with a mixture of ethyl acetate and hexane. The progress of the reaction was periodically monitored using <sup>1</sup>H and <sup>13</sup>C nuclear magnetic resonance (NMR) spectroscopy in CDCl<sub>3</sub>.

## Conclusions

In this study, we have successfully synthesized, crystallized, and characterized a novel amine-functionalized Ce(III) MOF (Ce-TPTC-NH<sub>2</sub>) and demonstrated its noteworthy efficiency in the catalytic conversion of CO2 into value-added cyclic carbonates. Single-crystal X-ray diffraction (SCXRD) confirmed its well-defined 3D crystalline structure, while spectroscopic

and adsorption studies validated the presence of accessible Lewis-acidic Ce(III) sites and uncoordinated (-NH<sub>2</sub>) groups. The TPD studies further validated the coexistence of both acidic and basic sites, which is pivotal in enhancing catalytic performance. The Ce-TPTC-NH2 MOF exhibited remarkable stability under catalytic conditions, achieving nearly quantitative conversion (98%). Furthermore, the catalyst demonstrated excellent stability and reusability, retaining ~90% of its activity after five consecutive cycles as confirmed by PXRD, HR-TEM, and MP-AES analysis. The cooperative interaction between the Lewis acidic cerium sites and the nucleophilic amine functionalities significantly enhances CO2 adsorption and activation, effectively overcoming the intrinsic thermodynamic and kinetic barriers associated with CO2 transformation. This synergistic effect is further validated by the reduced catalytic performance observed with the Ce-TPTC catalyst lacking the -NH<sub>2</sub> functionality. The mechanistic insights gained from this study provide a deeper understanding of structure-activity relationships in MOF-based catalysts for CO<sub>2</sub> fixation. Overall, our work contributes to the advancement of metal-organic frameworks in catalytic CO2 conversion and presents a promising strategy for sustainable carbon utilization, aligning with green chemistry principles for efficient CO2 valorization. Given the redox-active nature of cerium, Ce-TPTC-NH2 holds potential for photocatalysis, offering new avenues for light-driven CO2 conversion and sustainable transformations.

# **Author contributions**

Yogesh Kumar - original draft, methodology, investigation, formal analysis, and data curation. Rishukumar Panday single crystal data analysis, investigation, and formal analysis. Shaibal Banerjee - writing - review and editing, validation, supervision, resources, and conceptualization.

### Conflicts of interest

There are no conflicts to declare.

# Data availability

The data supporting this article have been included as part of the ESI.†

# Acknowledgements

This study was financially supported by the Defence Research and Development Organisation (DRDO). The author thanks Ramamoorthy Boomishankar, Department of Chemistry, Indian Institute of Science Education and Research, Pune, for providing crystal data support.

# References

Paper

- 1 M. Ding, R. W. Flaig, H.-L. Jiang and O. M. Yaghi, *Chem. Soc. Rev.*, 2019, **48**, 2783–2828.
- 2 K. Sumida, D. L. Rogow, J. A. Mason, T. M. McDonald, E. D. Bloch, Z. R. Herm, T.-H. Bae and J. R. Long, *Chem. Rev.*, 2012, 112, 724–781.
- 3 T. Jose, Y. Hwang, D.-W. Kim, M.-I. Kim and D.-W. Park, *Catal. Today*, 2015, **245**, 61–67.
- 4 W. N. Sit, S. M. Ng, K. Y. Kwong and C. P. Lau, *J. Org. Chem.*, 2005, **70**, 8583–8586.
- 5 F. Heshmatpour and R. Abazari, *RSC Adv.*, 2014, **4**, 55815–55826.
- 6 O. M. Yaghi, M. O'Keeffe, N. W. Ockwig, H. K. Chae, M. Eddaoudi and J. Kim, *Nature*, 2003, 423, 705–714.
- 7 H. Furukawa, K. E. Cordova, M. O'Keeffe and O. M. Yaghi, *Science*, 2013, **341**, 1230444.
- 8 M. J. Kalmutzki, N. Hanikel and O. M. Yaghi, *Sci. Adv.*, 2018, 4, eaat9180.
- 9 W. Lu, Z. Wei, Z.-Y. Gu, T.-F. Liu, J. Park, J. Park, J. Tian, M. Zhang, Q. Zhang and T. Gentle III, *Chem. Soc. Rev.*, 2014, 43, 5561–5593.
- 10 V. Guillerm, H. Jiang, D. Alezi, N. Alsadun and M. Eddaoudi, *Adv. Mater.*, 2024, 2414153.
- 11 F. Vermoortele, R. Ameloot, A. Vimont, C. Serre and D. De Vos, *Chem. Commun.*, 2011, 47, 1521–1523.
- 12 F. Vermoortele, M. Vandichel, B. Van de Voorde, R. Ameloot, M. Waroquier, V. Van Speybroeck and D. E. De Vos, *Angew. Chem., Int. Ed.*, 2012, **51**, 4887–4890.
- 13 H. Molavi, Coord. Chem. Rev., 2025, 527, 216405.
- 14 G. Ji, L. Zhao, J. Wei, J. Cai, C. He, Z. Du, W. Cai and C. Duan, *Angew. Chem., Int. Ed.*, 2022, **61**, e202114490.
- 15 K. Hendrickx, J. J. Joos, A. De Vos, D. Poelman, P. F. Smet, V. Van Speybroeck, P. Van Der Voort and K. Lejaeghere, *Inorg. Chem.*, 2018, 57, 5463–5474.
- F. Nouar, M. I. Breeze, B. C. Campo, A. Vimont, G. Clet,
   M. Daturi, T. Devic, R. I. Walton and C. Serre, *Chem. Commun.*, 2015, 51, 14458–14461.
- 17 Y. Zhang, H. Chen, Y. Pan, X. Zeng, X. Jiang, Z. Long and X. Hou, *Chem. Commun.*, 2019, 55, 13959–13962.
- 18 S. Dai, E. Montero-Lanzuela, A. Tissot, H. G. Baldoví, H. García, S. Navalón and C. Serre, *Chem. Sci.*, 2023, **14**, 3451–3461.
- 19 X.-P. Wu, L. Gagliardi and D. G. Truhlar, *J. Am. Chem. Soc.*, 2018, **140**, 7904–7912.
- 20 X. Han and M. Poliakoff, Chem. Soc. Rev., 2012, 41, 1428-1436.
- 21 D. Kim, D. W. Kim, O. Buyukcakir, M. K. Kim, K. Polychronopoulou and A. Coskun, *Adv. Funct. Mater.*, 2017, 27, 1700706.
- 22 A. Ma, F. Ke, J. Jiang, Q. Yuan, Z. Luo, J. Liu and A. Kumar, *CrystEngComm*, 2017, **19**, 2172–2177.
- 23 M. Lammert, M. T. Wharmby, S. Smolders, B. Bueken, A. Lieb, K. A. Lomachenko, D. De Vos and N. Stock, *Chem. Commun.*, 2015, 51, 12578–12581.

- 24 Y. Hu, R. Abazari, S. Sanati, M. Nadafan, C. L. Carpenter-Warren, A. M. Slawin, Y. Zhou and A. M. Kirillov, ACS Appl. Mater. Interfaces, 2023, 15, 37300–37311.
- 25 R. Abazari, S. Sanati, A. Morsali, A. M. Kirillov, A. M. Slawin and C. L. Carpenter-Warren, *Inorg. Chem.*, 2021, 60, 2056– 2067.
- 26 J. F. Kurisingal, Y. Rachuri, Y. Gu, R. K. Chitumalla, S. Vuppala, J. Jang, K. K. Bisht, E. Suresh and D.-W. Park, ACS Sustainable Chem. Eng., 2020, 8, 10822–10832.
- 27 S. Payra and S. Roy, *J. Phys. Chem. C*, 2021, **125**, 8497–8507.
- 28 J. X. Gu, H. Chen, Y. Ren, Z. G. Gu, G. Li, W. J. Xu, X. Y. Yang, J. X. Wen, J. T. Wu and H. G. Jin, *ChemSusChem*, 2022, 15, e202102368.
- 29 J. Senith Ravishan Fernando, S. S. Asaithambi and S. Maruti Chavan, *ChemPlusChem*, 2024, **89**, e202400107.
- 30 Q. Sun, H. Gao, M. Xiao, T. Sema and Z. Liang, *Environ. Sci. Technol.*, 2024, **58**, 10052–10059.
- 31 P. Gabrielli, M. Gazzani and M. Mazzotti, *Ind. Eng. Chem. Res.*, 2020, 59, 7033–7045.
- 32 C. C. Truong and D. K. Mishra, *J. CO*<sub>2</sub> *Util.*, 2020, **41**, 101252.
- 33 X.-H. Ji, N.-N. Zhu, J.-G. Ma and P. Cheng, *Dalton Trans.*, 2018, 47, 1768–1771.
- 34 J. Cai, H. Wang, H. Wang, X. Duan, Z. Wang, Y. Cui, Y. Yang, B. Chen and G. Qian, RSC Adv., 2015, 5, 77417– 77422.
- 35 W.-M. Liao, M.-J. Wei, J.-T. Mo, P.-Y. Fu, Y.-N. Fan, M. Pan and C.-Y. Su, *Dalton Trans.*, 2019, **48**, 4489–4494.
- 36 S. Yadav, N. Beniwal, G. Singh, P. Rekha and L. Singh, ACS Appl. Eng. Mater., 2024, 2, 2946–2961.
- 37 L. Chen, T. V. Janssens, M. Skoglundh and H. Grönbeck, *Top. Catal.*, 2019, **62**, 93–99.
- 38 A. Bavykina, N. Kolobov, I. S. Khan, J. A. Bau, A. Ramirez and J. Gascon, *Chem. Rev.*, 2020, **120**, 8468–8535.
- 39 Q. Yang, C. C. Yang, C. H. Lin and H. L. Jiang, *Angew. Chem.*, 2019, **131**, 3549–3553.
- 40 W.-L. Bao, J. Kuai, H.-Y. Gao, M.-Q. Zheng, Z.-H. Sun, M.-Y. He, Q. Chen and Z.-H. Zhang, *Dalton Trans.*, 2024, 53, 6215–6223.
- 41 C.-Y. Gao, J. Ai, H.-R. Tian, D. Wu and Z.-M. Sun, *Chem. Commun.*, 2017, 53, 1293–1296.
- 42 S. K. Das, S. Chatterjee, S. Bhunia, A. Mondal, P. Mitra, V. Kumari, A. Pradhan and A. Bhaumik, *Dalton Trans.*, 2017, 46, 13783–13792.
- 43 D. H. Le, R. P. Loughan, A. Gładysiak, N. Rampal, I. A. Brooks, A.-H. A. Park, D. Fairen-Jimenez and K. C. Stylianou, J. Mater. Chem. A, 2022, 10, 1442–1450.
- 44 J. Liang, R.-P. Chen, X.-Y. Wang, T.-T. Liu, X.-S. Wang, Y.-B. Huang and R. Cao, *Chem. Sci.*, 2017, **8**, 1570–1575.
- 45 Z.-Q. Li, Y.-Y. Zhang, Y.-J. Zheng, B. Li and G.-P. Wu, *J. Org. Chem.*, 2022, **87**, 3145–3155.
- 46 D. De, T. K. Pal, S. Neogi, S. Senthilkumar, D. Das, S. S. Gupta and P. K. Bharadwaj, *Chem. - Eur. J.*, 2016, 22, 3387–3396.